Acta Geologica Sinica (English Edition), 2020, 94(6): 2152–2164

Trace Elements in Sphalerite from the Dadongla Zn-Pb Deposit, Western Hunan–Eastern Guizhou Zn-Pb Metallogenic Belt, South China

HU Yusi[1, 2], YE Lin[1, *], WEI Chen[1, 2], LI Zhenli[1, 2], HUANG Zhilong[1] and WANG Haoyu[1, 2]

[1] *State Key Laboratory of Ore Deposit Geochemistry, Institute of Geochemistry, Chinese Academy of Sciences, Guiyang 550081, China*
[2] *University of Chinese Academy of Sciences, Beijing 100049, China*

Abstract: The western Hunan–eastern Guizhou Zn-Pb metallogenic belt is one of the important Zn-Pb mineralization regions in China. The Dadongla deposit, located in the northeast of Guizhou Province, is one of the typical Zn-Pb deposits in the region and has estimated resources more than 12 million metric tons (Mt) with an average grade of 4.11 wt% Zn+Pb. Its orebodies are hosted in the lower Cambrian Aoxi Formation dolomite, occurring as bedded, para-bedded in shape, and in conformity with the wall rock. The ore mineral assemblage is simple, dominated by sphalerite with minor pyrite and galena, and the gangue minerals are composed of dolomite, calcite with minor bitumen and barite. In view of the lack of geological and geochemical researches, the genesis of Zn-Pb ore is still unclear. Laser ablation-inductively coupled plasma mass spectrometry (LA-ICPMS) spot and mapping analyses were used to obtain sphalerite trace element chemistry in the Dadongla Zn-Pb deposit in Guizhou, China, aiming to constrain its ore genesis. The results show that sphalerite is characterized by the enrichment of Cd, Fe, Ge and Hg, corresponding with that of typical MVT deposits. Four zones were identified in the sphalerite crystal from Dadongla from the center to margin according to the color bands, in which the zone in the center, representing the early ore-stage sphalerite, is characterized by enrichment of Cd relatively, while the zone forming at late ore-stage is enriched in Ge and Hg relatively. The finding was controlled by differential leached metals content in ore-forming fluid from its source rock. Notably, critical element Ge trends to be enriched at the late ore-stage and follows a substitution of $2Zn^{2+} \leftrightarrow Ge^{4+}+\square$ (vacancy). Moreover, the calculated ore-forming temperature ranges from 79.9°C to 177.6°C by the empirical formula, which is similar to that of typical Mississippi Valley-type (MVT) deposits. Compared with the features of trace elements in sphalerite from different types of deposits, together with the geology, the Dadongla deposit belongs to an MVT Zn-Pb deposit.

Key words: trace elements, sphalerite, LA-ICPMS, MVT deposit, Western Hunan–Eastern Guizhou Zn-Pb metallogenic belt

Citation: Hu et al., 2020. Trace Elements in Sphalerite from the Dadongla Zn-Pb Deposit, Western Hunan–Eastern Guizhou Zn-Pb Metallogenic Belt, South China. Acta Geologica Sinica (English Edition), 94(6): 2152–2164. DOI: 10.1111/1755-6724.14616

1 Introduction

Sphalerite is one of the ubiquitous ore minerals in base metal sulfide deposits, including the volcanogenic massive sulfides (VMS), Mississippi Valley-type (MVT), sedimentary-exhalative (Sedex) and magmatic hydrothermal deposits (Höll et al., 2007; Cook et al., 2009). Commonly, Concentrates produced from Zn ore show significant enrichment of other elements, such as In and Ge, which are commonly extracted as an economic by-product during zinc smelting and refining (Alfantazi and Moskalyk, 2003; Höll et al., 2007). Other elements including Cd, Mn, Ga, Sn, Sb, Hg and Pb may also be enriched in sphalerite, if the concentrations are sufficiently high, it can also be economically exploited as a by-product.

Many remarkable papers have been published to deal with aspects of sphalerite (Oftedahl, 1940; Zhang, 1987; Pattrick et al., 1993; Cook et al., 2009; Ye et al., 2011; Frenzel et al., 2016; Lu et al., 2019; Wei et al., 2019). The seminal work of Oftedahl (1940) shows how trace elements content can be indicated the sphalerite formation temperature. Normally, Mn, Co and In are concentrated in the "high temperature" ores, while Ge, Ga and Cd are mainly enriched in the "low temperature" ores. Zhang (1987) proposed that trace element contents in sphalerite show significantly distinct in different ore genetic types and suggested that LnGa-LnIn and Zn/Cd-Se/Te-Ga/In diagrams can be used to distinguishing the genetic types of Zn-Pb deposits. Based on the electron beam techniques, the research from Pattrick et al. (1993) showed trace element contents are extremely inhomogeneous and present the μm-scale inclusions in sphalerite. Recently, the emerging LA-ICPMS analytic technique is playing a significant insight into the geochemical characteristic of sphalerite (Cook et al., 2009; Ye et al., 2011). Cook et al (2009) investigated the distribution trace elements (such as

* Corresponding author. E-mail: yelin@vip.gyig.ac.cn

Cd, Co, Ga, Ge, Pb, Sb, Bi, In and Mn) in sphalerite samples from 26 ore deposits, and confirmed that Cd, Co, Ga, Ge, In and Mn are present in solid solution and Pb, Sb and Bi mostly as micro-inclusions minerals. Ye et al. (2011) found that sphalerites from different ore genetic types in south China have significantly different trace element features, which can be used to discriminate the genetic types of Zn-Pb deposits. Recently, Frenzel et al. (2016) proposed a sphalerite GGIMFis geothermometer, which could be used to calculate the sphalerite formation temperature of various deposit types. Although a great number of studies have accessed the trace element contents in sphalerite to understand sphalerite geochemistry, the study of trace element partition in color zoned sphalerite is still scarce.

More than 500 different scale Zn-Pb deposits were distributed in the southeast margin of the Yangtze Block, but only a few studies have used the LA-ICPMS method to study trace elements in sphalerite (e.g., Ye et al., 2011, 2016; Yuan et al., 2018). The Dadongla deposit, located in the center of the western Hunan–eastern Guizhou Zn-Pb metallogenic belt, south China (Fig. 1a), is a typical middle-scale Zn-Pb deposit in eastern Guizhou and its Zn + Pb resources are more than 12 million metric tons (Mt) with an average grade of 4.11wt% Zn + Pb. Previous researchers are mainly focused on studying geological characteristics, ore-controlling factors and mining projects (e.g. Feng, 1995; Wang, 1996; Liao, 1999；Zhou et al. 2006). Whereas geochemical researches are relatively sparse, resulting in the origin of this deposit is still debated. Several remarkable studies have proposed various genetic models, including the stratabound deposits (Bao, 1987); the sedimentation-hydrothermal reformation (Wang, 1996), and Mississippi Valley-type (MVT) lead-zinc deposit model (Liao et al., 2015).

In this study, in-situ Laser ablation-inductively coupled plasma-mass spectrometry (LA-ICPMS) is used to investigate the sphalerite from Dadongla, aiming to (1) constrain the trace element partition in color zoned sphalerite, (2) calculate the sphalerite formation temperature and (3) discriminate the ore genetic type. The research not only provides new and accurate trace elements data of the deposit but also provide new geological and geochemical evidence for understanding the Zn-Pb mineralization in the western Hunan–eastern Guizhou Zn-Pb metallogenic belt.

2 Regional Geology

The western Hunan–eastern Guizhou Zn-Pb metallogenic belt, located in the western part of the Jiangnan regions, consists of Southeast Guizhou and northwest Hunan, which extends over 300 km (Fig. 1). In the area, the exposed rocks mainly consist of basement

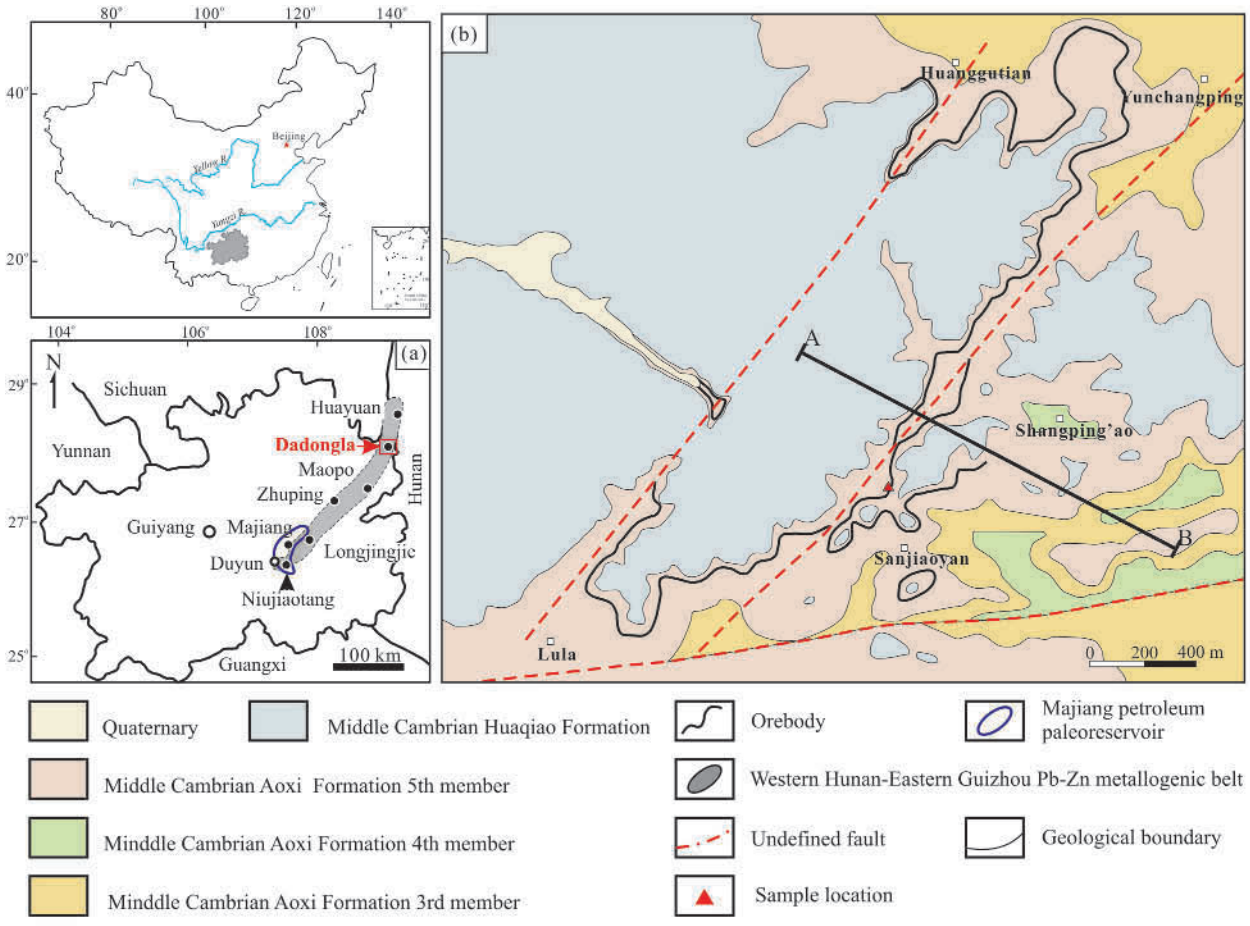

Fig. 1. (a) The location of the Dadongla deposit within China and the western Hunan–Eastern Guizhou metallogenic belt; (b) Geological map of the Dadongla deposit, with orebodies distribution and sample locations.

metamorphic rocks, sedimentary rocks, and minor igneous rocks. The basement includes the Neoproterozoic Banxi and Lengjiaxi groups and their equivalents which mainly consist of basalt interlayer with acidic volcanic rocks, tuff, tuffite, siltstone, quartz sandstone and silty shale, and has experienced weakly metamorphism. The Nanhua system comprises a series of continental sedimentary rocks, consisting of red clastic rock, siltstone, mudstone, moraine rock. Overlying sedimentary strata are the Ediacaran system to middle Triassic submarine carbonate and clastic sedimentary sequences in a passive continental margin, consisting of dolomite interlayer with minor shale/chert, carbonaceous mudstone, limestone and sandstone (Fig. 1). Upper Triassic to Cenozoic terrigenous sedimentary sequences are composed of red clastic rock, siltstone, black shale, and mudstone (Fig. 1). In addition, lamproite and kimberlite are sporadic emergences in the Kaili and Zhenyuan area of east Guizhou. It intrudes into the Lower Cambrian Qingxudong and Gaotai formations. Recent Sm-Nd and Rb-Sr dating wall rock indicate that the magmas emplaced between 497 and 503 Ma (Fang et al., 2002).

The western Hunan–eastern Guizhou area is subject to multistage tectonic events from the Neoproterozoic, Paleozoic and Mesozoic (Lu et al., 2005). The collision and amalgamation of Yangtze Block and the Cathaysia Block at 970–815Ma, corresponding to Jinning Orogeny, leading to the NE-trending tectonic framework was first established (Ren, 1996; Zhou et al., 2002; Pirajno, 2013). Subsequently, the Caledonian Orogeny at 513–386 Ma, forming several EW-trending shear zones(Ren, 1996; Zhou et al., 2002; Wang et al., 2007; Pirajno, 2013). During the Hercynian-Indosinian movements, the graben-type structure and local subsidence were controlled by two regional EW-trending shear zones (Ren, 1996; Zhou et al., 2002; Wang et al., 2005; Pirajno, 2013). During the Yanshanian period (Ren, 1996; Zhou et al., 2002; Hu and Zhou, 2012; Mao et al., 2013), the overlapped NW-trending structures were formed, overprinting the NE- and EW-trending structures, and occurred sinistral transpressional shear as a result of the oblique subduction of the Pacific Plate beneath the Asian continental plates. Additionally, a series of NE-trending and NNE-trending structures were developed by multistage tectonic events in this area. Those four regional faults, namely the Yinjiang–Huangyuan, the Songtao-Shiqian, the Yuping–Tongren–Baoqing and the Zhijiang–Xinhuang–Kaili regional faults, control the formation and distribution of the Zn-Pb deposits.

Those Zn-Pb deposits are mainly hosted in carbonate rock of the early Cambrian to Ordovician in age. Notably, over 90% of Zn-Pb deposits are hosted in the Lower Cambrian carbonate strata. Those deposits are characterized by stratiform ore, simple mineralogy, weak wall rock alteration, and low grade of Pb and Zn metals associated with the enrichment of Ag, Ge, Cd, Ga, and Hg. Recent, Rb-Sr dating sphalerite indicate that those carbonate-hosted Zn-Pb deposits occurred between 410 Ma to 490 Ma. This result shows the Zn-Pb mineralization in the western Hunan–eastern Guizhou area is related to the Caledonian orogenic event (e.g. Duan et al., 2014; Zhou et al., 2014; Yang et al., 2015).

3 Geology of the Dadongla Deposit

The Dadongla deposit is situated at the borders of the Guizhou and Hunan Province, 40 km northeast of Tongren city, Guizhou. Major faults in the area are dominated by the E-trending Saojiaoyan fault and the NE-trending Huanggutian fault. The Sanjiaoyan fault, which is characterized by a high dip angle (72°) and normal fault character, is over 3 km in length and 20 m in width. The Huanggutian fault, which is characterized by a high dip angle (75°) and normal fault character, is over 1 km in length and covered by regolith and vegetation.

The exposed strata in the Dadongla mining district range from Middle Cambrian Aoxi to Huqqiao formation (Fig. 2). The Middle Cambrian Aoxi Formation was divided into three members from bottom to top: (1) the 3rd member, predominantly composed of dark-grey to grey thin-bedded dolomite interlayer with black organic matter, argillaceous dolomite at the top part, 15 m in thickness; (2) the 4th member, composed of medium-bedded grey

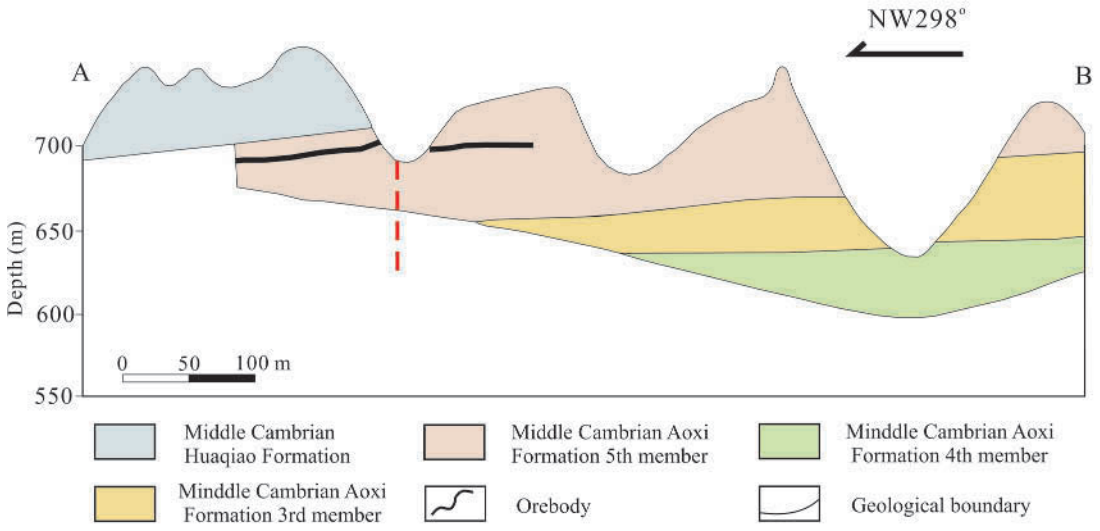

Fig. 2. Cross-section through the Dadongla deposit, revealing the distribution of orebodies, faults and strata.

dolomite, organic matter-bearing dolomite interlayer with dolorudite, 35–64 m in thickness; (3) the 5th member, which is the principal ore hosting sequence at the Dadongla deposit and it is predominantly composed of light grey to grey lamellar dolomicrite, argillaceous dolomite and finely crystalline dolomite and dolomicrite interlayer with cherts, 60–130 m in thickness. The Middle Cambrian Huaqiao Formation is overlain on the Middle Cambrian Aoxi Formation 5th member and is composed of black shale and interbed of grey argillaceous dolomite, calcitic dolomite and dolomite, 60 m in thickness.

The sulfide mineralization is epigenetic and occurs as massive fillings of horizontal and vertical karsts, veins and the vuggy porosity of dissolution of the host rocks. The Dadongla orefield includes two orebodies, named Orebody I and II (Fig. 2). The Orebody I occurs as stratiform or stratified and is in conformable contact with the wall rock. It is typically 2750 m in length and 600 m in width and 1.12–9.88 m in thickness (averaging 3.14 m in thickness). The ore grade of Zn + Pb of this orebody is between 1.42 and 14.85 wt% with the average ore grade of 4.11 wt%. The Orebody II is small in scale and remained in the middle to the upper part of an isolated mountain, and it is 2.45 m in thickness with the average ore grade of Zn + Pb 2.26 wt%.

Primary sulfide and supergene ore are observed in the Dadongla Zn-Pb deposit. Sulfide minerals are simple relatively and dominated by sphalerite with minor pyrite and galena (Figs. 3–4). Supergene ore is composed of smithsonite, hemimorphite and hydrozincite (Liao et al., 2015). The common gangue minerals are dolomite, calcite, with minor bitumen and barite (Figs. 3–4).

The ore structures are dominated by veins (Fig. 3a, c) and disseminated (Fig. 3b, d). The principal ore textures are euhedral-subhedral to subhedral-anhedral granular, fragmented texture and metasomatic relict texture. The granular texture is the most common. Sphalerite is characteristically coarse-grained, euhedral-subhedral granular and granular in shape (50–500 μm), which enclose pyrite (Fig. 4a–b), or wrapped by dolomite and calcite (Fig. 4a–b), and most sphalerite is light yellow in color (Fig. 4d–f). Galena is euhedral-subhedral granular, and the individual grains are 100–500 μm in diameter and have cubic cleavage (Fig. 4c), which is enclosed by dolomite (Fig. 4c). Pyrite is fine-grained (10–50 μm), and is commonly enclosed by sphalerite ores (Fig. 4a–b). In addition, calcite and dolomite fill in the vug and facture of sulfides (Fig. 4).

According to the mineral assemblages and crosscutting relationship of the Dadongla deposit, three ore-stage

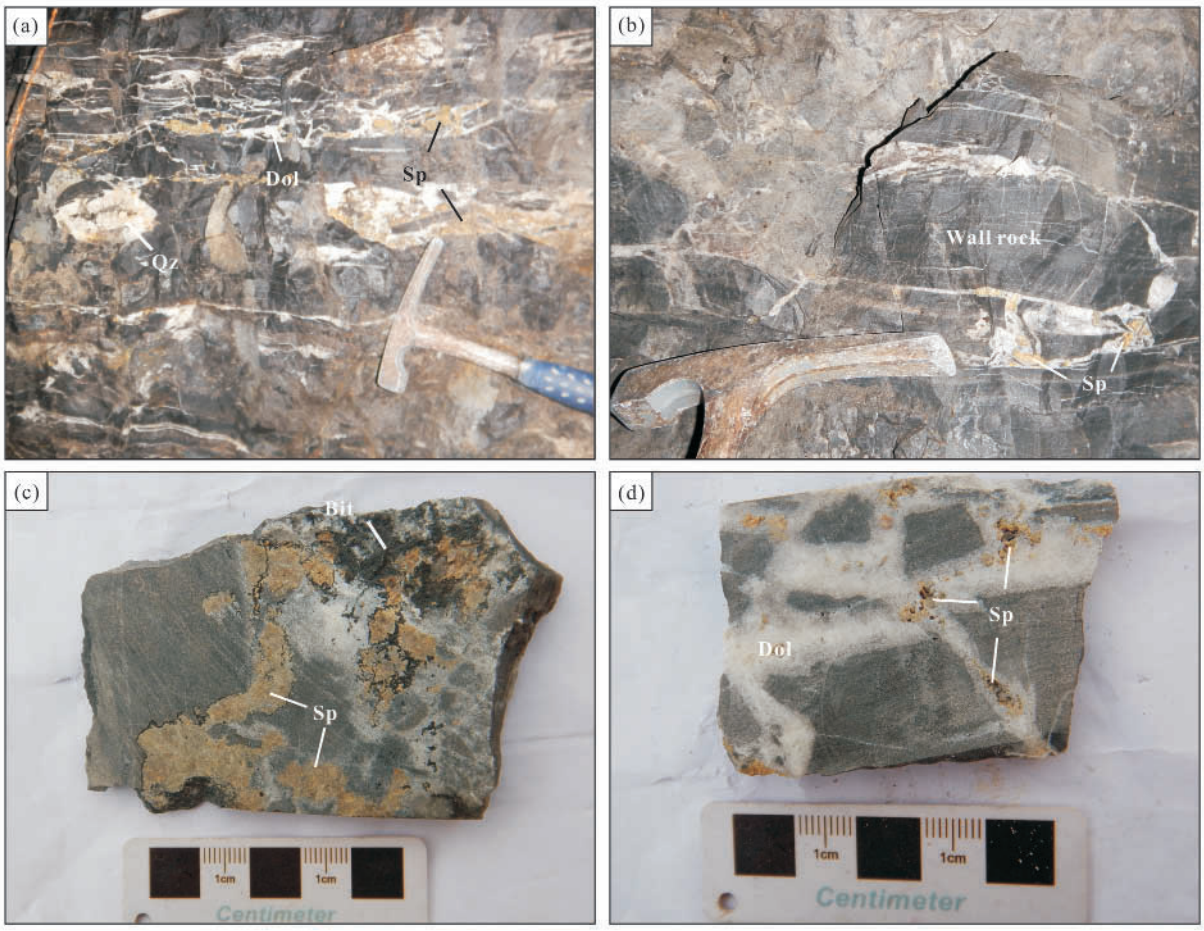

Fig. 3. Mineral assemblages and textures of the samples from the Dadongla deposit.
(a) Stockwork of sphalerite and hydrothermal dolomite cemented the fragments of dolostone; (b) fine-grain sphalerite fill in the facture of dolostone; (c) sphalerite and bitumen distributed in the fragments of the host rock; (d) sphalerite-hydrothermal dolomite assemblage filled in the fracture of the dolostone. Abbreviations: Sp-Sphalerite; Gn-galena; Py-pyrite; Dol-dolomite; Bit-Bitumen; Qz-quartz.

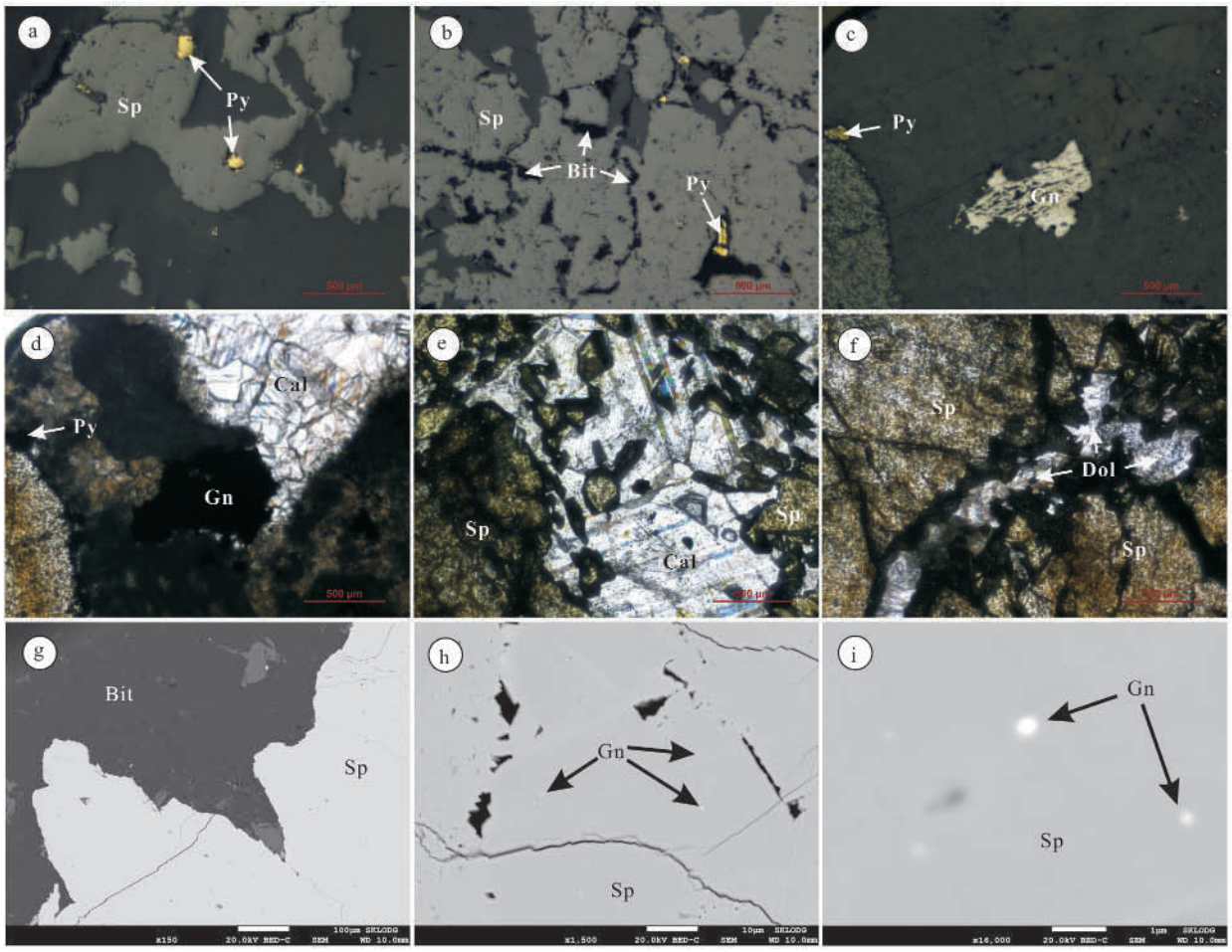

Fig. 4. Photomicrographs of representative samples from the Dadongla deposit.
(a) Sphalerite replaced or enclose pyrite; (b) bitumen distributes in the facture of coarse-grained sphalerite; (c) galena intergrowth with calcite; (d) galena wrapped by pyrite and hydrothermal dolomite;. (e) calcite fill in the vug of euhedral sphalerite granule; (f) hydrothermal dolomite fill in the facture of sphalerite; (g) bitumen distributes in the wall rock surrounding sphalerite; (h) galena inclusion appears in sphalerite; (i) galena inclusion in sphalerite. Photomicrographs a–c were taken under reflected plane-polarized light, d–f were taken under transmitted plane-polarized light, and g-i were taken under backscattered electron mode of scanning electron microscopy. Abbreviations: Sp-Sphalerite; Gn-galena; Py-pyrite; Dol-dolomite; Cal-calcite; Bit-bitumen.

successive stages of mineralization in the deposit were established, including: (1) Stage I, it is the pre-ore forming stage, and the pyrite formed mainly in the stage, in which the fine-grained euhedral pyrite is disseminated within the wall rock, accompanied with minor hydrothermal dolomite; (2) Stage II, it belongs to main Zn-Pb ore-forming stage, accounting for at least 90 vol.% of the total sphalerite resource. The sphalerite and hydrothermal dolomite with minor galena and bitumen formed at the stage; (3) Stage III, it is a late ore-stage of mineralization, bitumen, hydrothermal dolomite and calcite formed at this stage. Normally, the bitumen occurs in a limited fracture network with sphalerite and hydrothermal dolomite in the ore area. The paragenetic sequence in the Dadongla deposit is concluded in Fig. 5.

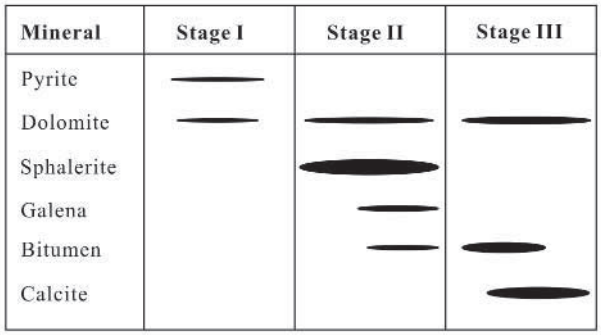

Fig. 5. Mineral paragenesis of the Dadongla deposit.

4 Sampling and Methods

The ore-bearing samples were collected from the mining adit of Dadongla. The spot locations selected for LA-ICPMS analysis were biased towards coarse-grained sphalerite generally free of visible inclusions. Backscattered electron images analyzed by scanning electron microscopy was used to feature the samples, paying particular attention to compositional inhomogeneity, micro-inclusions, zoning, or other textural

aspects, all of which may influence trace element distributions. Trace element in sphalerite was conducted by LA-ICPMS at the State Key Laboratory of Ore Deposit Geochemistry, Institute of Geochemistry, Chinese Academy of Sciences (IGCAS). Laser sampling was performed using an ASI RESOLution-LR-S155 laser microprobe equipped with a Coherent Compex-Pro 193 nm ArF excimer laser. An Agilent 7700x ICP-MS instrument was used to acquire ion-signal intensities. Helium (350 ml/min) was applied as a carrier gas. The ablated aerosol was mixed with Ar (900 ml/min) as a transport gas, before exiting the cell. Each analysis incorporated a background acquisition of approximately 30 s (gas blank) followed by 60 s of data acquisition from the sample. Analyses were run with 26 μm pit size, 5 Hz pulse frequency and 3 J/cm^2 fluence.

Each sample was measured Zn content by EMPA to be used as the internal standard. While STDGL3 was used to determine concentrations of chalcophile and siderophile elements (Danyushevsky et al., 2011). The preferred values of element concentrations for the USGS reference glasses are from the GeoReM database (http://georem.mpch-mainz.gwdg.d e/). Sulfide reference material MASS-1 was analyzed as unknown sample to check the analytical accuracy.

5 Results

5.1 Distribution features of trace elements in sphalerite

The results of minor and trace elements in sphalerite from the Dadongla deposit are listed in Table 1. Fe and Cd show significantly high concentrations in sphalerite from this deposit, ranging from 811 to 20750 ppm and 5193 to 30585 ppm with the mean contents of 10167 ppm and 12250 ppm respectively. Sphalerite from this deposit display relatively higher Ge, Pb and Hg contents with wide concentration ranges. In which, Ge content varies from 126 to 1162 ppm, averaging 600 ppm, and Pb and Hg contents range are 57.2–4541 ppm and 174–10248 ppm with the mean content of 857 and 2821 ppm respectively. Except for the above-mentioned trace elements, only Mn and Ga contents are more than 100 ppm, varying from 5.81 to 260 ppm and 3.41 to 191 ppm and their mean contents are 91.4 ppm and 32.0 ppm, respectively. Other trace element contents are significantly <10 ppm. For example, Cu was detected in 31 spots, ranging from 0.30 to 15.2 ppm with a mean concentration of 4.30 ppm, and In is present in 39 spots with contents up to 3.37 ppm. As, Ag and Sb were detected varying from 1.27 to 28.7 ppm, 0.68 to 5.72 ppm and 0.03 to 21.0 ppm with means concentration of 11.68 ppm, 2.47 ppm and 5.97 ppm, respectively. Co was detected only in 2 spots with concentrations of 0.23 and 0.24 ppm. Additionally, Cr, Mo, W, Au and Bi are mostly lower than the limit of detection.

5.2 Distribution features of trace elements in color zone sphalerite

At the scale of individual crystal, four zones can be classified by significantly different colors, and evident chemical variations can be observed at this crystal-scale in sphalerite from Dadongla (Fig. 6). Zone I is characterized by light-yellow to yellow semicircular core with a 1.44 mm radius. Zone II has a maximum thickness of 5 mm and a minimum of 1 mm, and displays shades of brown. Zone III is a rim of Zone II about 0.5 mm in width and Zone IV appearing to be on the margins of Zone III, is hunter green with a thickness ranging from 0.5 to 1.5 mm.

The trace element dataset in sphalerite is composed of 8 spots measured in Zone I, 16 spots measured in Zone II, 8 spots measured in Zone III and 8 spots measured in Zone IV, for a total of 40 spots analyses including two traverses (Fig. 6). Interestingly, trace elements, in particular Fe, Cd, Ge, Hg, show clear variations among different zones. Fe regarded as one of the most dominating trace elements in sphalerite fluctuates within a range from 811 to 20750 ppm of two traverses, which display that Fe contents in those four zones are floating and inhomogeneous. Cd, considered as a primary trace element in sphalerite, shows an obvious distinction among those four color bands. Cd concentrations of two traverses show that its contents in Zone I are more about 1500 ppm than that in the other three zones, which means Zone I is characterized by high Cd content. Ge and Hg are secondary trace elements in sphalerite from Dadongla, and their contents of two traverses exhibit an increasing trend from Zone I to Zone IV, especially up to the top in Zone IV. Meanwhile, Pb contents of those two traverses fluctuate in varying degrees. SEM analysis shows the high Pb content in sphalerite, indicating some spots with special high Pb content may include galena inclusion (Fig. 4h–i). Except few spots with high Pb contents, Pb contents of two traverses manifest a slight rising from Zone I to Zone IV.

Despite low concentrations of Cu, As, Ag and Sb, those trace elements also increasing from the center to margin of the sphalerite, show an enriched trend in Zone IV. Specifically, Zone I, the center of the sphalerite crystal, is characterized by an enrichment of Cd, while Zone IV, the margin of the sphalerite crystal, is more enriched in Ge, Hg, Cu, Ag, As and Sb. Fe and Pb do not indicate an obvious increasing or decreasing trend in sphalerite from the Dadongla Zn-Pb deposit.

6 Discussion

6. 1 Ore-forming temperature

Many researchers suggested that the trace element features in sphalerite are related to the ore-forming temperature, such as higher-temperature systems generally characterized by high In, Cu and Sn, while Ge and Cd enriched belonging to lower-temperature systems (Ye et al., 2011). Sphalerite forming under high temperature is enriched in Fe, Mn, In, Se and Te with high In/Ga ratio, whereas sphalerite is characterized by high Cd, Ga and Ge contents and low In/Ge ratio under low temperature (Liu et al., 1984; Cai et al., 1996; Ye et al., 2016). Thus, given sphalerite from Dadongla Zn-Pb deposit relatively with high Cd and Ge concentrations, this deposit possibly formed under low temperature. Moreover, Frenzel et al. (2016) further studied the relation between trace elements in sphalerite and the ore-forming temperature, maintaining that sphalerite from different deposit types has obvious

Table 1 LA-ICPMS data of trace elements (ppm) in sphalerite from Dadongla deposit

Spot	Mn	Fe	Cu	Ga	Ge	As	Ag	Cd	In	Sn	Sb	Hg	Pb
Zone I													
Spot-1	8.69	811	-	6.70	404	3.24	2.84	19726	0.12	0.48	0.65	216	143
Spot-2	31.2	18218	0.55	44.2	214	9.18	0.99	8247	1.12	1.32	3.65	477	364
Spot-3	7.78	7261	-	70.6	236	2.42	1.93	21363	0.51	0.93	1.39	232	85.9
Spot-4	5.88	5352	0.30	191.4	151	1.85	3.01	23649	1.24	0.47	0.48	248	67.7
Spot-5	9.32	8614	0.30	90.2	126	2.25	2.16	30585	0.20	0.42	2.02	659	66.9
Spot-6	5.81	2066	0.31	39.4	250	1.72	3.08	26012	0.30	0.32	0.47	240	89.5
Spot-7	9.38	8898	0.32	49.3	154	1.51	1.73	25861	0.06	0.74	1.28	304	74.4
Spot-8	6.63	9488	0.48	11.2	207	1.27	1.01	20207	0.63	1.56	2.28	467	57.2
Min	5.81	811	0.30	6.70	126	1.27	0.99	8247	0.06	0.32	0.47	216	57.2
Max	31.2	18218	0.55	191.4	404	9.18	3.08	30585	1.24	1.56	3.65	659	366
Mean	10.6	7589	0.38	62.9	217	2.93	2.09	21956	0.52	0.78	1.53	355	119
Zone II													
Spot-9	35.7	18857	0.40	6.76	313	7.36	0.89	6290	0.09	0.30	0.14	225	362
Spot-10	42.1	16630	0.91	3.41	367	5.90	1.47	10481	0.01	0.39	0.08	376	379
Spot-11	53.3	16065	0.41	6.52	512	9.19	1.05	10542	0.01	0.37	0.12	213	508
Spot-12	67.8	9865	0.67	5.65	577	6.83	1.31	8506	-	0.47	0.62	375	729
Spot-13	211	2266	0.96	32.8	822	11.2	3.10	6858	0.21	0.55	0.80	499	3680
Spot-14	49.5	13331	-	95.4	453	4.40	1.30	11288	0.33	0.27	0.03	176	468
Spot-15	28.6	13363	0.43	42.1	337	11.0	1.09	8553	1.45	9.67	9.47	1614	254
Spot-16	175	2742	0.80	18.2	516	11.75	1.48	5193	0.96	4.37	5.58	759	3404
Spot-17	50.1	18682	-	10.2	319	8.71	0.78	7424	0.13	0.54	0.52	175	397
Spot-18	59.1	18295	-	3.53	516	10.76	0.68	10792	0.02	0.48	0.08	174	513
Spot-19	26.5	14821	-	7.26	368	5.17	0.72	10722	0.02	0.32	-	183	275
Spot-20	110	4255	0.86	21.4	1033	12.0	1.36	8017	0.24	0.73	0.30	581	1650
Spot-21	260	1757	-	4.76	837	12.5	2.10	6904	0.10	0.39	0.94	174	4541
Spot-22	158.8	6070	-	4.50	650	10.1	1.04	6076	0.08	0.85	1.21	267	2791
Spot-23	54.2	9368	1.77	19.6	654	13.9	1.56	8904	2.55	2.07	3.51	1904	772
Spot-24	66.4	9050	1.79	18.2	574	10.8	1.58	8918	3.37	3.55	5.94	1766	831
Min	26.5	1757	0.40	3.41	313	4.40	0.68	5193	0.01	0.27	0.03	174	254
Max	260	18857	1.79	95.4	1033	13.9	3.10	11288	3.37	9.67	9.47	1904	4541
Mean	90.5	10964	0.90	18.8	553	9.48	1.35	8467	0.64	1.58	1.95	591	1347
Zone III													
Spot-25	130	4430	-	5.71	712	10.4	0.82	5599	0.05	-	0.08	216	2095
Spot-26	149	15388	10.5	21.3	912	28.7	4.61	8077	0.83	3.33	14.2	8336	860
Spot-27	95.9	20750	3.87	17.0	692	19.9	2.40	5193	1.17	4.62	8.76	4918	851
Spot-28	96.7	13271	5.18	43.7	604	21.0	3.12	8372	2.08	3.87	8.34	6789	761
Spot-29	163	17868	15.2	33.9	656	18.0	5.72	11817	2.42	6.56	18.6	10248	520
Spot-30	151	11887	11.5	65.0	702	23.0	4.97	7773	1.49	5.10	21.0	8058	740
Spot-31	26.2	4227	3.86	21.1	261	5.88	3.07	13658	1.38	5.87	15.1	1182	192
Spot-32	53.4	5229	0.74	13.6	448	6.23	1.20	10537	0.94	1.20	1.44	613	839
Min	26.2	4227	0.74	5.71	261	5.88	0.82	5193	0.05	1.20	0.08	216	192
Max	163	20750	15.2	65.0	912	28.7	5.72	13658	2.42	6.56	21.0	10248	2095
Mean	108	11631	7.26	27.7	623	16.6	3.24	8878	1.29	4.36	10.9	5045	857
Zone IV													
Spot-33	138	11636	7.67	19.0	981	20.3	3.54	12382	1.67	4.14	15.7	7606	816
Spot-34	175	9784	9.40	15.6	1042	19.5	4.43	13678	0.10	1.88	10.4	8136	988
Spot-35	194	5690	11.59	23.1	1115	19.1	5.12	12494	2.75	5.43	16.8	9145	1087
Spot-36	207	6689	11.26	25.4	1165	23.5	4.98	12840	1.97	5.04	16.5	9179	1546
Spot-37	107	17470	5.14	6.52	1106	21.1	4.61	15224	0.17	1.34	4.48	2111	2084
Spot-38	152	13027	7.89	17.1	1048	20.3	3.98	15859	0.26	2.06	9.02	6365	1019
Spot-39	157	9001	10.63	40.6	985	18.6	4.14	13587	1.85	4.59	16.4	7498	867
Spot-40	127	4189	7.65	106	1001	16.8	3.85	11800	2.23	5.90	14.7	10155	980
Min	107	4189	5.14	6.52	981	16.8	3.54	11800	0.10	1.34	4.48	2111	816
Max	207	17470	11.59	106	1165	23.5	5.12	15859	2.75	5.90	16.8	10155	2084
Mean	157	9686	8.90	31.7	1055	19.9	4.33	13483	1.37	3.80	13.0	7524	1173

differences in Fe, Ga, Ge, In and Mn contents and those trace elements concentrations could result in a number correlating strongly with the homogenization temperature of fluid inclusions through statistical analysis. This number could be expressed as $PC1^*=\ln\left(\frac{C_{Ga}^{0.22}\cdot C_{Ge}^{0.22}}{C_{Fe}^{0.37}\cdot C_{Mn}^{0.20}\cdot C_{In}^{0.11}}\right)$, and the empirical relationship between this number and the homogenization temperature is expressed as $T(°C)= -(55.4 \pm 7.3)\cdot PC1^* + (208 \pm 10)$. Based on that formula, the ore-forming temperature of several Zn-Pb deposits have been calculated according to trace element concentrations in sphalerite, such as Nayongzhi Zn-Pb deposit (100.5–164.4° C in accordant with the homogenization temperature of fluid inclusions in sphalerite 102.1–155.2° C, Wei et al., 2018). Similarly, considering the lack of study on the homogenization temperature of fluid inclusions in Dadongla, the ore-forming temperature of this deposit could be obtained using the empirical formula, listed in Table 2. The results indicate that the ore-forming temperature of sphalerite from the Dadongla Zn-Pb deposit ranges from 79.9 to 177.6°C, which falls into the

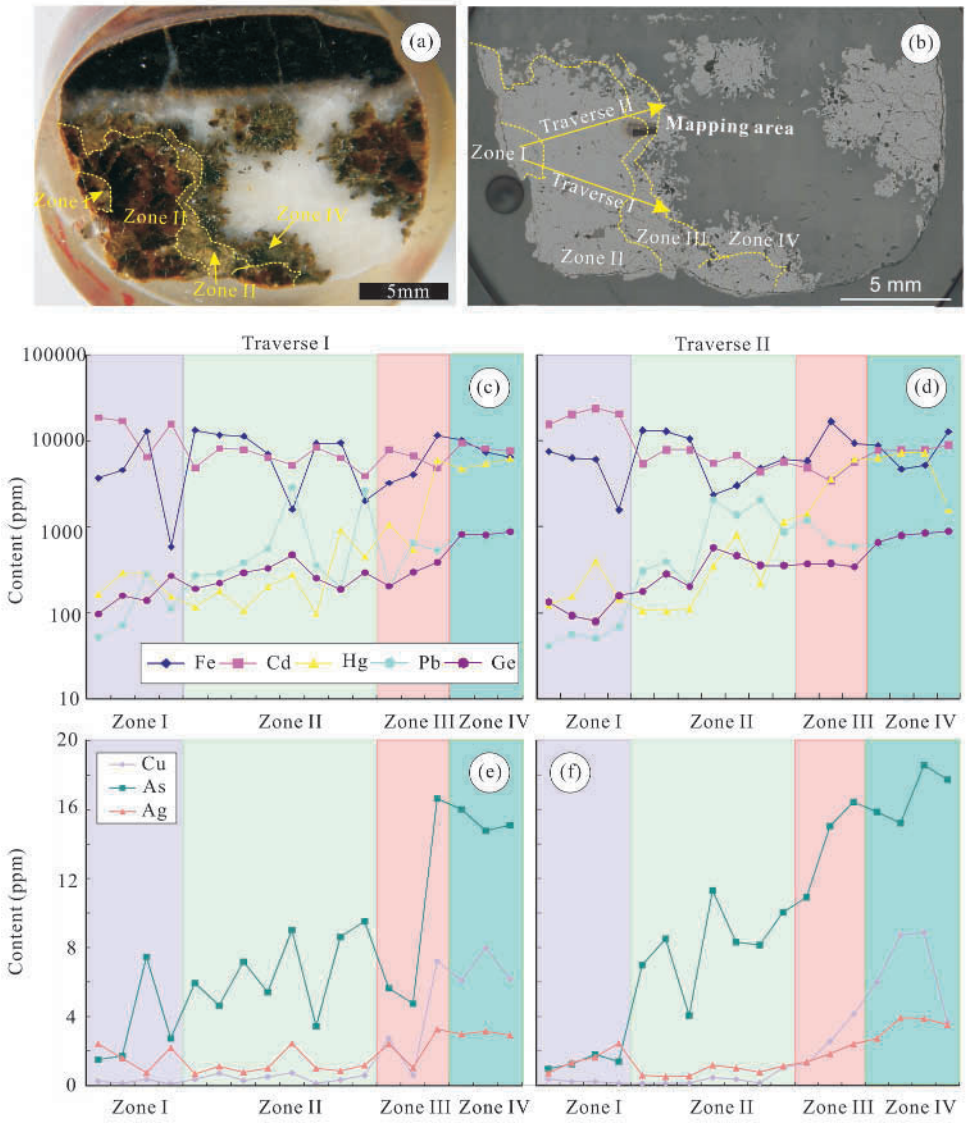

Fig. 6. Images and trace element contents of the color zoned sphalerite.
(a) Hand specimen photos of the color zoned sphalerite investigated in this study; (b) the color zoned sphalerite under reflected plane-polarized light; (c) variation of Fe, Cd, Hg, Pb and Ge in traverse I; (d) Variation of Fe, Cd, Hg, Pb and Ge in traverse II; (e) variation of Cu, As and Ag in traverse I; (f) variation of Cu, As and Ag in traverse II.

range of MVT deposit (Fig. 7), and is also accordant with the homogenization temperature of fluid inclusion of a typical MVT deposit (90~150°C, Leach et al., 2005). Interestingly, different colored zones show distinct temperature ranges and range from 79.9 to 166.8°C in Zone I (avg. 105.76°C), 81.4 to 171.5°C in Zone II (avg. 136.0°C), 104.2 to 177.6°C in Zone III (avg. 143.3°C) and 86.6 to 170.7°C in Zone IV (avg. 138.3°C). Despite a slight increase in average temperature from Zone I to IV, their ranges of temperature are similar, especially the max temperature. Namely, there are no significant differences between the ore-forming temperature of sphalerite forming early and late, but considering the ranges, early and late sphalerite formed under almost the same temperature.

6.2 Controlling trace elements variations in color zone sphalerite

Trace elements such as Fe, Cd, Ge, Cu, Pb, and other elements, can partition from hydrothermal fluids and be incorporated into sphalerite lattice by substituting Zn^{2+} during crystal growth (Cook et al., 2009; Ye et al., 2011; Gagnevin et al., 2014). In this study, each color zone in sphalerite shows clear different trace element composition, which helps to assess the extent of fluid variation during sphalerite growth. The fluctuation of Fe and Hg in color zone sphalerite suggests that metals in hydrothermal fluids are inhomogeneous. A similar conclusion can be reached in the Mapping image (Fig. 8). The inner sphalerite zone displays a different geochemical signature (i.e., higher Cd) to sphalerite in the out part of the color zone (i.e., higher Ge, Hg, Cu, Ag, As and Sb). Previous studies show that the distribution of individual metals in sphalerite critically depends on the extent of metal leach from its source rock (Viet al., 1992; Gagnevin et al., 2014) or shift the growth environment (i.e., changes in temperature) during crystal growth. As mentioned above, the ore-forming temperature

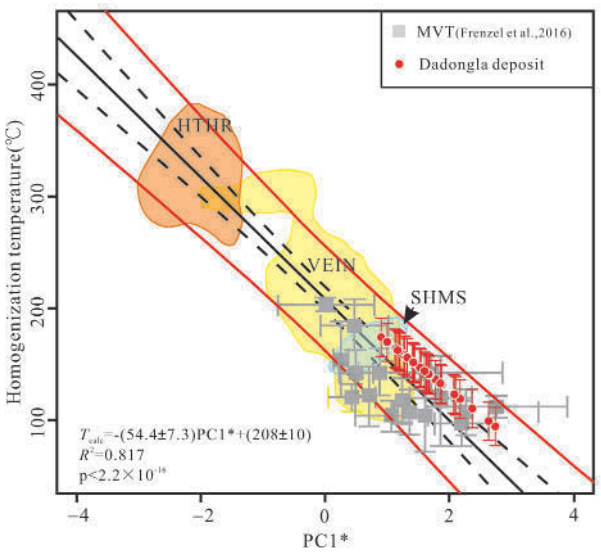

Fig. 7. Representative time-resolved depth profiles for sphalerite from the Dadongla deposit by LA-ICPMS.

is largely overlapped, which suggests temperature change is unlikely as the main factor for controlling trace elements variation in sphalerite. Thus it shows that differential leaching and extracting metals from source control the hydrothermal fluid carrying those metal concentrations and further lead to the inhomogeneous distribution of trace elements in sphalerite crystal.

6.3 Critical element Ge occurrence in sphalerite

Previous studies suggested that Ge^{2+} directly substitutes Zn^{2+} (Bernstein, 1985; Johan, 1988; Cook et al., 2009), Ge^{2+} and Cu^{2+} substitutes Zn^{2+} (Ye et al., 2016) or $2Zn^{2+}\leftrightarrow Ge^{4+}+Cu^{+}$ (Belissont et al., 2016). Despite there is no direct correlation between Cu and Ge in the mapping area (Fig. 8), their contents of two traverse lines show a similar increasing trend from the center to margin of sphalerite and Fig. 9, including the comparison between Ge and Cu concentrations of all data, displays a faint positive correlation between Ge and Cu. Otherwise, Cu contents are significantly lower than Ge contents, which could impossibly support the following substitution mechanisms: $3Zn^{2+}\leftrightarrow 2Cu^{+}+Ge^{4+}$. But increasing Cu concentration elevates the incorporation of Ge during Dadongla sphalerite precipitate from hydrothermal fluid (Johan, 1988). A similar case has been reported in sphalerite from the Lehong deposits, south China (Wei et al., 2019). Considered with the flat signal of Ge in Fig. 10, Ge does not occur in sphalerite as micro-inclusion. Moreover, K-edge X-ray absorption near edge spectra (XANES) suggests the Ge occurs as Ge^{4+} in the tetravalent site of Ge-rich sphalerite from Tres Marias, Mexico (Cook et al., 2015). Similar oxidation of Ge has been proposed for sphalerite from Saint-Salvy deposit, France by Belissont et al. (2016). Thus, we consider that the Ge^{4+} occurs in the sphalerite from the Dadongla deposit, which supports a substitution such as $2Zn^{2+}\leftrightarrow Ge^{4+}+\square$ (vacancy).

6.4 Genetic type of deposit

Many researchers have studied the features of trace elements in sphalerite from different types of Zn-Pb deposits, and compared the trace element contents in sphalerite from those Zn-Pb deposits (Cook et al., 2009; Ye et al., 2011, 2012, 2016). Those researches showed that different types of Zn-Pb deposits have significantly different characteristics of trace elements in sphalerite. For example, magmatic hydrothermal deposits are enriched in Fe, Mn, In, Sn and Co with low Cd, Ge and Ga (such as Bainiuchang deposit in Yunnan, China; Ye et al., 2011); VMS deposit is characterized by high Fe, Mn and In contents but low Cd, Ge and Ga contents (such as Laochang deposit in Yunnan, China; Ye et al., 2011); Skarn is enriched in Mn and Co, depleting In, Sn and Fe (such as Hetaoping deposit in Yunnan; Ye et al., 2011); And sphalerite of MVT is characterized by enrichment of Cd, Ge, Ga and depleted in Fe, Mn, In, Sn and Co (such as Niujiaotang Zn-Cd deposit in Guizhou, China; Ye et al., 2011). Thus, comparing the features of trace elements in sphalerite from different types of deposits, the results suggest that Mn, In, Sn and Co are closely related to the magma system, while Cd and Ge are commonly enriched

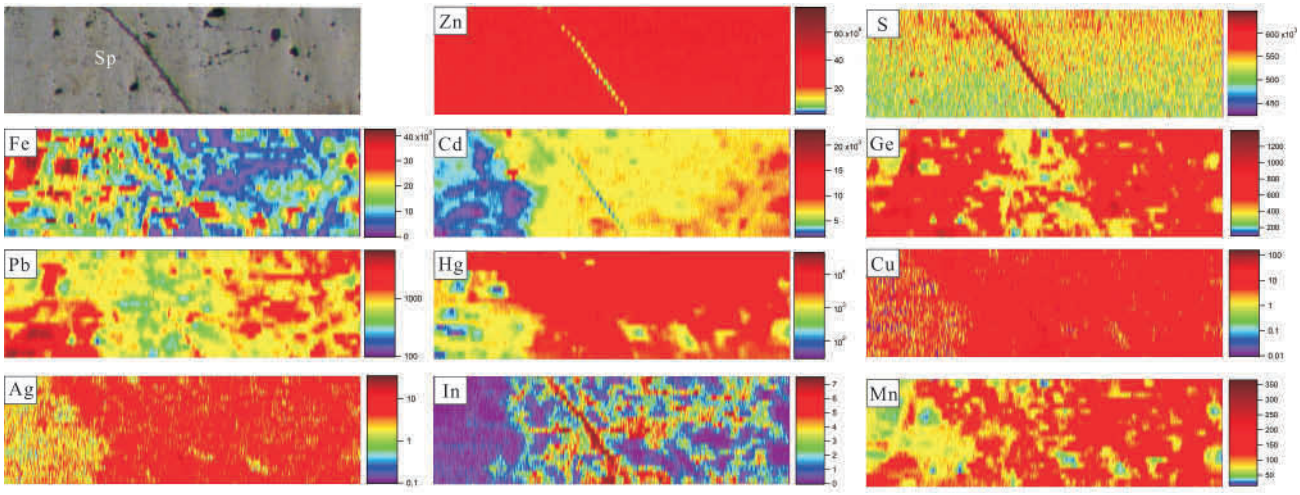

Fig. 8. Elemental maps generated with LA-ICPMS show the distribution of selected trace elements in sphalerite from the Dadongla deposit.

Table 2 Ore-forming temperature of the Dadongla deposit calculated by the GGIMFis geothermometer

Spot	PC1*	Max (℃)	Min (℃)	Mean (℃)
Zone I				
Spot-1	2.47	102.2	-	84.2
Spot-2	1.09	166.8	130.8	148.8
Spot-3	1.92	127.9	79.9	103.9
Spot-4	2.11	118.9	-	93.5
Spot-5	1.84	131.8	84.9	108.3
Spot-6	2.39	106.1	-	88.6
Spot-7	1.87	130.1	82.8	106.5
Spot-8	1.40	152.5	112.1	132.3
Zone II				
Spot-9	1.00	171.0	136.3	153.7
Spot-10	1.18	162.5	125.2	143.8
Spot-11	1.30	157.2	118.3	137.7
Spot-13	1.90	129.1	81.4	105.2
Spot-14	1.59	143.7	100.5	122.1
Spot-15	1.28	157.8	119.0	138.4
Spot-16	1.46	149.4	108.1	128.7
Spot-17	0.99	171.5	137.0	154.2
Spot-18	1.04	169.2	133.9	151.6
Spot-19	1.34	155.0	115.3	135.1
Spot-20	1.73	136.7	91.3	114.0
Spot-21	1.61	142.6	99.1	120.9
Spot-22	1.20	161.7	124.2	142.9
Spot-23	1.20	161.6	124.0	142.8
Spot-24	1.10	166.4	130.4	148.4
Zone III				
Spot-25	1.49	147.9	106.1	127.0
Spot-26	1.03	169.5	134.5	152.0
Spot-27	0.86	177.6	145.0	161.3
Spot-28	1.14	164.5	127.9	146.2
Spot-29	0.87	177.1	144.4	160.8
Spot-30	1.25	159.4	121.2	140.3
Spot-31	1.52	146.5	104.2	125.4
Spot-32	1.37	153.9	113.9	133.9
Zone IV				
Spot-33	1.07	168.1	132.5	150.3
Spot-34	1.36	154.3	114.5	134.4
Spot-35	1.28	158.0	119.4	138.7
Spot-36	1.27	158.3	119.7	139.0
Spot-37	1.01	170.7	136.0	153.4
Spot-38	1.20	161.6	124.1	142.8
Spot-39	1.29	157.4	118.6	138.0
Spot-40	1.81	133.0	86.6	109.8

in “low-temperature” deposits. Based on that summary, the distribution of trace elements in sphalerite from the Dadongla Zn-Pb deposit is compared with different types of Zn-Pb deposits. The results show that sphalerite from Dadongla Zn-Pb deposit is enriched in Cd, Ge but depleted in In, Co and Ni, according to the feature of “low -temperature” deposits. Binary plots of In vs. Mn in sphalerite suggests that sphalerite from the Dadongla Zn-Pb deposit is characterized by lower In and Mn contents than epithermal, skarn, VMS, and magmatic hydrothermal deposits, similar to the range of MVT deposits (Fig. 11). Moreover, Ag and Ge concentrations are also applied to contrasting the Dadongla deposit to different genetic type deposits (Fig. 11), indicating that sphalerite from the Dadongla deposit is enriched in Ge and depleted Ag in accordant with the feature of MVT deposits, especially Ge significantly higher than that of the other genetic type deposits. Hence, the feature of trace elements in sphalerite from the Dadongla deposit is similar to that of MVT deposits.

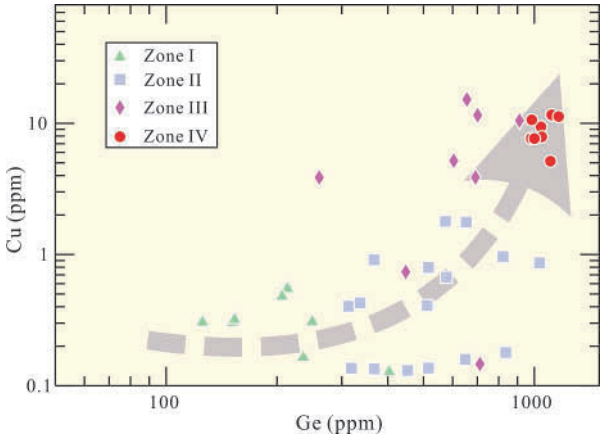

Fig. 9. The diagram of Ge-Cu for sphalerite of the Dadongla deposit.

In fact, the geological features from Dadongla are also similar to that of MVT deposits, including: (1) the Zn-Pb orebodies are bedded, para-bedded and in conformity with the strata, showing obvious epigenetic mineralization; (2) no intrusion have been found in the area, indicating the Zn -Pb mineralization has no genetic association with intrusive rocks; (3) the ore mineral assemblage is very simple, consisting of sphalerite with minor galena and pyrite; (4) low grade of Zn and Pb, commonly lower than 5%; (5) the ore-forming temperature belong to low temperature (< 150° C). Overall, the geological and geochemical evidence suggests that the Dadongla Zn-Pb deposit is an MVT deposit.

7 Conclusion

Sphalerite from the Dadongla Zn-Pb deposit is characterized by high Cd, Fe, Ge, Hg, which can be divided into four zones from the center to margin on the basis of the different color bands. Zone forming at the early ore-stage is characterized by enrichment of Cd, while zone forming at the late ore-stage is enriched in Ge and Hg.

According to the empirical formula, the ore-forming temperature varies from 79.9 to 177.6°C, which is similar to the homogenization temperature of fluid inclusion in the typical MVT deposit.

(3) The inhomogeneous distribution of trace elements in sphalerite crystal was controlled by the extent of metal contents in ore-forming fluid leaching from its source rock.

(4) Sphalerite from this deposit are plotted into MVT ranges in the binary plots of Ge vs. Mn and In vs. Co. Combined with its geological feature, the ore-forming temperature and sphalerite trace elements geochemistry, it is suggested that the Dadongla Zn-Pb deposit belongs to an MVT Zn-Pb deposit.

Acknowledgments

This research project was supported by the National

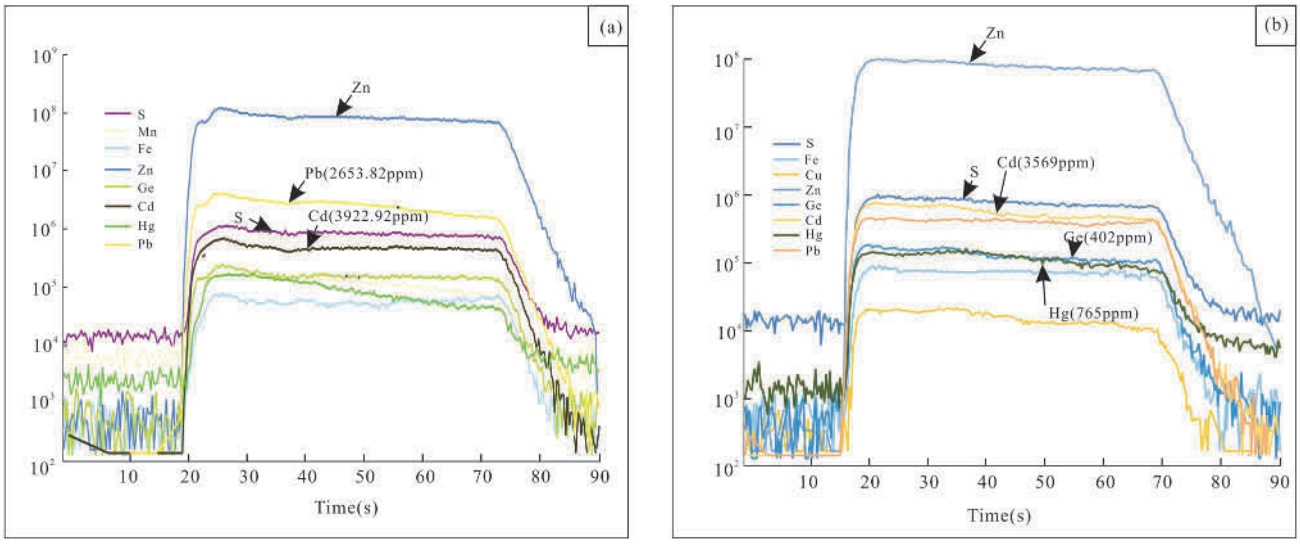

Fig. 10. The homogenization temperature of the Dadongla deposit showing the GGIMFis geothermometer (modified after Frenzel et al. 2016).

The line of best fit is shown as the black line; 95% confidence intervals are shown as the black dotted lines and the prediction intervals of linear fit are shown as the red lines.

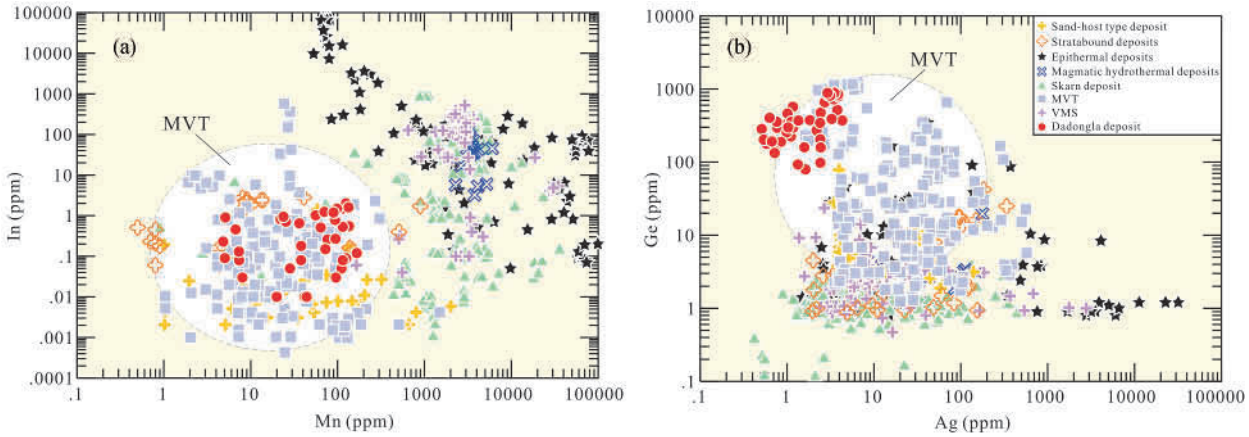

Fig. 11. Binary plots of Mn vs. In (a) and Ag vs. Ge (b) in sphalerite from the Dadongla deposit and other Zn-Pb deposits from China, NE Europe, and Japan.

The plots are based on data from Cook et al. (2009), Ye et al. (2011, 2016).

Natural Science Foundation of China (41673056 and U1812402), the Key Program of Guizhou Natural Science Foundation (Qiankehejichu [2017]1421), the State Key Program of National Natural Science Foundation of China (41430315), and National Key R&D Program of China (2017YFC0602500). We would like to thank Dr. Zhihui Dai (State Key Lab. of Ore Deposit Geochemistry, Institute of Geochemistry) for her assistance in LA-ICPMS analysis. We express our appreciation to two anonymous reviewers for their insightful comments that greatly improved the quality of the manuscript.

Manuscript received May 21, 2019
accepted Oct. 24, 2019
associate EIC: XU Jifeng

edited by FEI Hongcai

References

Alfantazi, A.M., and Moskalyk, R.R., 2003. Processing of indium: a review. Minerals Engineering, 16: 687–694.

Bao, Z.X., 1987. Metallogenic Mechanism of Mercury-Lead-Zinc Deposits in Western Hunan and Eastern Guizhou. Journal of Guilin College of Geology, 7(8): 159–170 (in Chinese with English abstract).

Belissont, R., Muñoz, M., Boiron, M.C., Luais, B., and Mathon, O., 2016. Distribution and oxidation state of Ge, Cu and Fe in sphalerite by μ-XRF and K-edge μ-XANES: insights into Ge incorporation, partitioning and isotopic fractionation. Geochimica et Cosmochimica Acta, 177: 298–314.

Bernstein, L. R., 1985. Germanium geochemistry and mineralogy. Geochimica et Cosmochimica Acta, 49(11): 2409–2422.

Cai, J.H., Zhou, W.N., and Zhang, J.Z., 1996. Typomorphic characteristics of sphalerites in the Yinshan Copper, Lead and

Zinc polymetallic deposit, Jiangxi. Journal of Guilin Institute of Technology, 16(4): 370–375 (in Chinese with English abstract)

Cook, N.J., Ciobanu, C.J., Pring, A., Skinner, W., Shimizu, M., Danyushevshky, L., Saini-Eidukat, B., and Mecher, F., 2009. Trace and minor elements in sphalerite: A LA-ICPMS study. Geochim. Cosmochim. Acta, 73: 4761–4791.

Cook, N. J., Etschmann, B., Ciobanu, C., Geraki, K., Howard, D., Williams, T., Rae, N., Pring, A., Chen, G., Johannessen, B., and Brugger, J., 2015. Distribution and substitution mechanism of Ge in a Ge-(Fe)-bearing sphalerite. Minerals, 5 (2): 117–132.

Danyushevsky, L., Robinson, P., Gilbert, S., Norman, M., Large, R., McGoldrick, P., and Shelley, M., 2011. Routine quantitative multi-element analysis of sulphide minerals by laser ablation ICP-MS: standard development and consideration of matrix effects. Geochemistry: Exploration, Environment, Analysis, 11: 51–60.

Duan, Q.F., Gao, L., Zeng, J.K., Zhou, Y., Tang, Z.Y., and Li, K., 2014. Rb-Sr dating of sphalerite from Shizishan Pb-Zn deposit in Huayuan ore concentration area, western Hunan, and its geological significance. Earth Science–Journal of China University Geosciences, 38(8): 977–999 (in Chinese with English abstract).

Fang, W.X., Hu, R.Z., Su, W.C., Xiao, J.F., Qi, L., and Jiang, G.H., 2002. The emplacement age of lamproite in the Zhenyuan district, Guizhou. Chinese Science Bulletin, 47(4): 307–312 (in Chinese with English abstract).

Feng, X.S., 1995. A discussion on possibility of seeking for Pb-Zn deposits in the Dadongla Mercury field, Eastern Guizhou. Guizhou Geology, 12(3): 204–207 (in Chinese with English abstract).

Frenzel, M., Hirsch, T., and Gutzmer, J., 2016. Gallium, germanium, indium, and other trace and minor elements in sphalerite as a function of deposit type—A meta-analysis. Ore Geology Reviews, 76(9):52–78.

Gagnevin, D., Menuge, J.F., Kronz, A., Barrie, C., and Boyce. A., 2014. Minor elements in layered sphalerite as a record of fluid origin, mixing, and crystallization in the Navan Zn-Pb ore deposit, Ireland. Economic Geology, 109: 1513–1528.

Höll, R., Kling, M., and Schroll, E., 2007. Metallogenesis of germanium—a review. Ore Geology Reviews, 30: 145–180.

Hu, R.Z., and Zhou, M.F., 2012. Multiple Mesozoic mineralization events in South China- an introduction to the thematic issue. Mineralium Deposita, 47: 579–588.

Johan, Z., 1988. Indium and germanium in the structure of sphalerite: an example of coupled substitution with copper. Mineralogy and Petrology, 39: 211–229.

Leach, D.L., Sangster, D.F., Kelley, K.D., Large, R.R., Garven, G., Allen, C.R., Gutzmer, J., and Walters, S., 2005. Sediment-hosted lead-zinc deposits: a global perspective. In Economic Geology. 100th Anniversary, 561–607.

Liao, Z.W., 1999. Feature and genesis of zinc deposit in Dadongla Mercury Orefield. Guizhou Geoloy, 16(4): 315–320 (in Chinese with English abstract).

Liao, Z.W., Wang, S.W., Sun, X.M., Jiang, X.F., Zhou, Q., Xu, X.Y., and Guo, Y., 2015. Rb-Sr dating of sphalerites from MVT Pb-Zn deposits in northeastern Guizhou Province and geological implications. Mineral Deposits, 34(4): 769–785 (in Chinese with English abstract).

Liu, Y.J., Cao, M.L., Li, Z.L., Wang, H.N., and Chu, T.Q., 1984. Geochemistry of Element. Beijing: Science Press, 1–548 (in Chinese).

Lu, H.Z., Wang, Z.G., Wu, X.Y., Chen, W.Y., Zhu, X.Q., Guo, D.J., Hu, R.Z., and Keita, M., 2005. Turbidite-hosted gold deposits in SE Guizhou Province, China: their regional setting, structural control and gold mineralization. Acta Geologica Sinica, 79(1): 98–105 (in Chinese with English abstract).

Lu, S.Y., Ren, T.S., Yang, Q., Sun, Z.M., Hao, Y.J., and Sun, X.H., 2019. Ore genesis for stratiform ore bodies of the Dongfengnanshan Copper Polymetallic Deposit in the Yanbian area, NE China: Constraints from LA-ICP-MS in situ trace elements and sulfide S-Pb isotopes. Acta Geologica Sinica (English Edition), 93(5): 1591–1606.

Mao, J.W., Cheng, Y.B., Cheng, M.H., and Pirajno, F., 2013. Major types and time-space distribution of Mesozoic ore deposits in South China and their geodynamic settings. Mineralium Deposita, 48: 267–294.

Oftedahl, I., 1940. Untersuchungen über die Nebenbestandteile von Erzmineralien norwegischer zinkblendführender Vorkommen. Skrift. Norsk Vidensk. Akad. Oslo, Math. Naturv. Kl., 8:1–103.

Pattrick, R.A.D., Dorling, M., and Polya, D.A., 1993. TEM study of indium-bearing and copper-bearing growth-banded sphalerite. Canadian Mineralogist, 31: 105–117.

Pirajno, F., 2013. The geology and tectonic settings of China's mineral deposits. Springer Dordecht, 9–11.

Ren, J.S., 1996. The continental tectonics of China. Journal of Southeast Asian Earth Sciences, 13: 197–204.

Viets, J.G., Hopkins, R.T., and Miller, B.M., 1992. Variations in minor and trace-metals in sphalerite from Mississippi Valley-type deposits of the Ozark Region: Genetic implications: Economic Geology, 87: 1897–1905.

Wang, H.Y., 1996. A genetic model for mineralization of the Zinc -Lead belts in Eastern Guizhou. Guizhou Geology, 13(1): 7–23 (in Chinese with English abstract).

Wang, Y.J., Zhang, Y.H., Fan, W.N., and Peng, T.P., 2005. Structural signatures and $^{40}Ar/^{39}Ar$ geochronology of the Indosinian Xuefenshan tectonic belt, south China block. Journal of Structural Geology, 27: 985–998.

Wang, Y.J., Fan, W.M., Zhao, G.C., Ji, S.C., and Peng, T.P., 2007. Zircon U-Pb geochronology of gneissic rocks in the Yunkai massif and its implications on the Caledonian event in the South China block. Gondwana Research, 12: 404–416.

Wei, C., Huang, Z.L., Yan, Z.F., Hu, Y.S., and Ye, L., 2018. Trace element contents in sphalerite from the Nayongzhi Zn-Pb deposit, northwestern Guizhou, China: Insights into incorporation mechanisms, metallogenic temperature and ore genesis. Minerals, 8(11): 490.

Wei, C., Ye, L., Hu, Y.S., Danyushevsky, L., Li, Z.L., and Huang, Z.L., 2019. Distribution and occurrence of Ge and related trace elements in sphalerite from the Lehong carbonate-hosted Zn-Pb deposit, northeastern Yunnan, China: Insights from SEM and LA-ICP-MS studies. Ore Geology Reviews, doi.org/10.1016/j.oregeorev.2019 .103175

Yang, H.M., Liu, C.P., Duan, R.C., Gu, X.M., Lu, S.S., Tan, J.J., Cai, Y.X., Zhang, L.G., and Qiu, X.F., 2015. Rb-Sr and Sm-Nd isochron ages of Bokouchang Pb-Zn deposit in Tongren, Guizhou Province and their geologcial implication. Geotectionic et Metallogenia, 39(5): 855–865 (in Chinese with English abstract).

Ye, L., Cook, N.J., Ciobanu, C.L., , Liu, Y.P., Zhang, Q., Liu, T.G., Gao, W., Yang, Y.L., and Danyushevskiy, L., 2011. Trace and minor elements in sphalerite from base metal deposits in South China: A LA-ICPMS study. Ore Geology Reviews, 39 (4): 188–217.

Ye, L., Gao, W., Yang, Y.L., and Liu, T.G., and Peng, S.S., 2012. Trace elements in sphalerite in Laochang Pb-Zn polymetallic deposit, Lancang, Yunnan Province. Acta Petrologica Sinica, 28(5): 1362–1372 (in Chinese with English abstract).

Ye, L., Li, Z.L., Hu, Y.S., Huang, Z.L., Zhou, Z.J., Fan, H.F., and Danyushevskiy, L., 2016. Trace element in sulfide from Tianbaoshan Pb-Zn deposit, Sichuan Province, China: A LA-ICPMS study. Acta Petrologica Sinica, 32(11): 3377–3393 (in Chinese with English abstract).

Yuan, B., Zhang, C.Q., Yu, H,J., Yang, Y.M., Zhao, Y.X., Zhu, C.C., Ding, Q.F., Zhou, Y.B., Yang, J.C., and Xu, Y., 2018. Element enrichment characteristics: Insights from element geochemistry of sphalerite in Daliangzi Pb-Zn deposit, Sichuan, Southwest China. Journal of Geochemical Exploration, 186: 187–201.

Zhang, Q., 1987. Trace elements in galena and sphalerite and their geochemical significance in distinguishing the genetic types of Pb–Zn ore deposits. Chinese Journal of Geochemistry, 6: 177–190.

Zhou, M.P., and Zhu, D.W., 2006. Application of the High-density Induced Polarization (IP) for Exploration of the Dadongla Mercury- zinc Deposit in Northeast of Guizhou Province. Guizhou Geology, 23(4): 312–322 (in Chinese with English abstract).

Zhou, T.H., Goldfarb, R.J., and Phillips, G.N., 2002. Tectonics and distribution of gold deposits in China- an overview. Mineralium Deposita, 37: 249–282.

Zhou, Y., Duan, Q.F., Tang, J.X., Cao, L., Li, F., Huang, H.L., and Gan, J.M., 2014. The large-scale low-temperature mineralization of lead-zinc deposits in western Hunan: Evidence from fluid Inclusions. Geology and Exploration, 50 (3): 515–532 (in Chinese with English abstract).

About the first author

HU Yusi, female, born in 1993 in Chongqing City; Ph.D candidate; studying in State Key Laboratory of Ore Deposit Geochemistry, Institute of Geochemistry, Chinese Academy of Sciences. She now focuses on studying the genesis of Zn-Pb deposits in Western Hunan–Eastern Guizhou. Email: huyusi@mail.gyig.ac.cn.

About the corresponding author

YE Lin, male, born in 1970 in Guizhou Province; master; graduated from Nanjing University University; research fellow of State Key Laboratory of Ore Deposit Geochemistry, Institute of Geochemistry, Chinese Academy of Sciences. He is now interested in the study on trace elements in sulfides from different genetic types of Zn -Pb deposits. Email: yelin@vip.gyig.ac.cn.